Supporting Information

Turnquist et al. 10.1073/pnas.1407898111

SI Materials and Methods

Mouse Colonies. Apoptosis-stimulating protein of p53 with signature sequences of ankyrin repeat-, SH3 domain-, and proline-rich region-containing protein 2 (*ASPP2*) Δexon3 mutant mice were generated on a mixed C57BL/6Jx129SvJ background and backcrossed in a BALB/c background for nine generations. *ASPP2* Δexon3 mutant mice were genotyped as described in previous studies (1) using the following primers: 5′-CTCCACCCCAGGAAATTACA-3′ (intron 3), 5′-CGGTTTGGAAGTCAAAGGAA-3′ (exon 3), and 5′-GGACCGCTATCAGGACATA-3′ (neomycin resistance gene).

Middle Cerebral Artery Occlusion Experimental Stroke. The middle cerebral artery (MCA) occlusion model was induced by 30 min of left-sided intraluminal filament occlusion as a model of transient focal cerebral ischemia as previously described (2, 3). We inserted a surgical filament into the external carotid artery and threaded it forward into the internal carotid artery until the tip occluded the origin of the MCA, resulting in a cessation of blood flow and subsequent brain infarction in the MCA territory. After 50 min, the filament was removed, and the MCA was reperfused. Animals were recovered in heated incubators for 12 h, and body temperature kept at 35–36 °C.

Theiler's Murine Encephalomyelitis Virus Infection. PFU BeAN 8386 virus was suspended in 0.03 mL sterile HBSS and injected into the right posterior cortex through a 27-gauge needle. Injections were localized to a point halfway to midline at ear level into the right posterior cerebellar cortex. Sham mice received injections of 0.03 mL HBSS. Theiler's murine encephalomyelitis virus viral production and infection were performed in accordance with previous studies (4, 5).

Maternal Inflammation Model. An i.p. injection of 0.01 mg/kg LPS (*Escherichia coli* 055:B5; Sigma-Aldrich) was made in female C57BL/6 mice at embryonic day 13.5 (6). Age-matched control animals were injected with an equal volume of saline. Animals were killed by cervical dislocation (dams) or decapitation (fetuses) 8 d after LPS injection. All animal procedures were conducted in line with United Kingdom Home Office approval (license number 30/2524).

LPS Injection Model. An i.p. injection of 10 mg/kg LPS or saline (055:B5; Sigma-Aldrich) was made in female BALB/c mice at postnatal day 20. Age- and sex-matched controls were injected with an equal volume of LPS or saline ($n = 4$). Animals were killed 24 h after LPS injection. All animal procedures were conducted in line with United Kingdom Home Office approval (license number 30/2524).

Patient Samples. Human temporal cortex and age- and region-matched inflammatory disease tissues were obtained from the Thomas Willis Oxford Brain Bank. For immunostaining experiments, three cases of subacute/chronic encephalitis of presumed viral etiology, three cases of cerebral infarct, and three region-matched control cases were used. Experiments involving human tissue were carried out in accordance with the Human Tissue Act and the Codes of Practice from the Human Tissue Authority and received ethics approval under the project title "ASPP in normal and diseased brain" (Thomas Willis Oxford Brain Bank Request 74; full ethics: Xin Lu: 09/0606/78).

Tissue Immunohistochemistry and Immunofluorescence. Tissue sections were washed in PBS before blocking for 1 h in PBS containing 0.1% Triton-X and 10% donkey serum (Sigma). Donkey serum is used to block nonspecific binding sites before incubation with primary antibody overnight at 4 °C. Antigens were detected using the antibodies listed in Table S1. After overnight incubation, they were washed in PBS three times for 10 min before incubation with the appropriate conjugated secondary antibodies for 1 h at room temperature (RT). The secondary antibody was conjugated to fluorophores Alexa-488, -568, and -647 (1:400; Invitrogen). After washing in PBS three times for 10 min, sections were incubated for 10 min in DAPI (10 μg/mL; Sigma-Aldrich) to counterstain the cell nuclei and rinsed three times for 10 min in 0.1 M phosphate buffer. Sections were mounted, and slides were coverslipped with FluorSave mounting medium (Chemicon). Omission of primary antibody was used as a negative control in all immunofluorescence experiments. For immunohistochemistry on paraffin sections, slides were heated to 65 °C before immersion in histoclear and rehydration with graded alcohols. Sections were blocked in 1% H_2O_2 in PBS-Tween 20 and then, 5% normal goat serum in PBS-Tween 20. Antigens were detected using the antibodies listed in Table S1. Binding of the primary antibody was detected using a biotinylated secondary antibody listed in Table S2 with an ABC Standard Kit (Vector Laboratories). Visualization was enabled using a 0.05% diaminobenzene hydrochloride solution (Sigma). Omission of primary antibody was used as a negative control in all immunohistochemistry experiments.

Immunoblotting. Cell lines were grown in 100-cm dishes, washed with PBS, and lysed in urea buffer (8 M urea, 1 M thiourea, 0.5% CHAPS, 50 mM DTT, 24 mM spermine). Lysates were kept on ice for 30 min before sonication. Protein concentration was measured using the Bradford assay method. NuPAGE 4× loading buffer was added to all lysates and then boiled for 5 min; 30–100 μg protein was loaded onto an SDS polyacrylamide gel for electrophoresis, and proteins were then transferred onto a nitrocellulose membrane. Membranes were blocked in 5% milk in Tris-Buffered Saline (125 mM Tris, 200 mM NaCl) containing 0.1% Tween 20. Membranes were incubated in the primary antibodies listed in Table S1 overnight at 4 °C and washed three times in Tris-Buffered Saline-Tween 20. Membranes were then incubated in secondary antibody (Table S2) for 1 h at RT, and the signal was visualized using ECL detection (Amersham Biosciences) using X-ray films (Fujifilm).

RNA Extraction and cDNA Preparation. mRNA was extracted using the RNeasy Mini Kit (Qiagen) according to the manufacturer's instructions. For mouse brain tissue, 10–20 mg frozen cortical tissue was added to 300 μL lysis buffer containing 0.001% β-mercaptoethanol. Tissues or cells were homogenized, and lysate was mixed 1:1 with 70% ethanol and centrifuged through an RNeasy Mini Spin column. The column was washed and treated with DNase 1 for 15 min before washing again to remove contaminants. RNA was eluted with RNase-free water. The abundance and quality of the resulting RNA were assessed using a Nanodrop ND-1000 spectrophotometer (Nanodrop Technologies). RNA samples were diluted so that 200 ng total RNA could be used for a 25-μL reverse-transcription reaction. cDNA was synthesized using SuperScript II Reverse Transcriptase (Invitrogen).

Quantitative Real-Time PCR. For the quantitative analysis of mRNA expression, the Tecan Sunrise 7500 Real-Time PCR System (Applied Biosystem) was used with the DNA binding dye SYBR Green (Qiagen) for the detection of PCR products. Each reaction was performed in triplicate using 1 μL cDNA in a final volume of 25 μL. The following thermal cycle was used for all samples: 10 min at 95 °C and 40 cycles of 30 s at 95 °C, 40 s at primer-specific annealing temperatures, and 40 s at 72 °C. The melting points, optimal conditions, and specificities of the reactions were first determined using a standard procedure. Quantitative RT-PCR was performed using the gene-specific primers listed in Table S3. The expression level of each target gene was analyzed based on the ΔΔCt method, and the results are expressed as relative expression corrected to the housekeeping gene GAPDH.

Cell Culture and RNAi. Mouse embryonic fibroblasts were prepared and cultured as described previously (7) from ASPP2 Δexon3 mice. The murine macrophage cell line RAW264.7, the murine microglial cell line BV-2, and HEK 293T cells (ATCC) were maintained in DMEM (GIBCO; Invitrogen) with 10% heat-inactivated FBS (GIBCO), 5% penicillin, and 5% streptomycin. Primary human astrocytes (ScienCell) were maintained in astrocyte medium (ScienCell). THP-1 cells (ATCC) were maintained in RMPI-1640 (GIBCO; Invitrogen) with 10% FBS, 0.05 mM 2-mercaptoethanol, 2 mM L-glutamine, 10 mM Hepes, and 1 mM sodium pyruvate. Cells were plated at 1×10^5 cells/mL and treated with LPS (1 μg/mL; *E. coli* 055:B5; Sigma-Aldrich) or left untreated at time points up to 24 h after treatment.

siRNA oligos against mouse ASPP2, human and mouse p65, and human and mouse signal transducer and activator of transcription 1 (STAT1) were purchased from Dharmacon. Sequences are available from Dharmacon or on request. We used siGENOME RISC-Free siRNA (Dharmacon) as a negative control. THP-1 cells were transfected with the indicated siRNA oligos at a final concentration of 35 nM using Dharmafect 1 reagent (Dharmacon) according to the manufacturer's instructions. For siRNA-mediated knockdowns in RAW264.7 cells, Amaxa Nucleofection Kit V was used according to the manufacturer's instructions.

Cellular Immunofluorescence. Cells were washed with PBS and fixed for 10 min with 4% paraformaldehyde. Cells were permeabilized with 0.01% Triton-X for 4 min, washed with PBS, and then blocked in 5% FBS for 1 h at RT. Primary antibodies listed in Table S1 were applied overnight at 4 °C. Cells were washed with PBS before incubation with a secondary antibody conjugated to fluorophores Alexa-488, -568, and -647 (1:500; Invitrogen Paisley) and DAPI (1:2,000) for 30 min. Coverslips were mounted on slides with FluorSave mounting medium (Chemicon). Omission of primary antibody was used as a negative control in all immunocytochemistry experiments.

ChIP Assay. ChIP assays were performed using the SimpleChIP Enzymatic Chromatin IP Kits (Cell Signaling Technology) as per the manufacturer's instructions. Briefly, RAW264.7 cells with indicated treatments were incubated for 10 min with 1% formaldehyde solution at RT followed by incubation with 125 mM glycine. Antibodies used for the murine ChIP were as follows: rabbit anti-Stat1 (sc-345x; Santa Cruz Biotechnology) and normal rabbit IgG. Six fragments of the sequence 1,058 bp upstream and 195 bp downstream of the murine ASPP2 promoter transcription start site (TSS) were assayed for in vivo binding by STAT1. Then, three distinct fragments of the sequence 765–398 bp upstream of the ASPP2 promoter TSS were assayed for in vivo binding by STAT1. Additionally, THP-1 cells with indicated treatments were incubated for 10 min with 1% formaldehyde solution at RT followed by incubation with 125 mM glycine. Antibodies used for the human ChIP were as follows: rabbit anti-STAT1 (9172; Cell Signaling Technology) and normal rabbit IgG. Eight fragments of the sequence 1,126 and 367 bp downstream of the human ASPP2 promoter TSS were assayed for in vivo binding by STAT1. DNA fragments were quantified by quantitative RT-PCR using the primers listed in Table S4.

Luciferase Constructs. The human ASPP2 promoter sequence −1,126 to −964 was amplified from human genomic DNA by PCR with forward primer 5′-TCGATGGAGATTCTGGTAAGGG-3′ and reverse primer 5′- TGTTCTAGTAAGTTGTCAGTGCA-3′. The human ASPP2 promoter sequence −992 to −882 was amplified from human genomic DNA by PCR with forward primer 5′-TGAACTTGCACTGACAACTTACT-3′ and reverse primer 5′-AAAGAGTAGCAGAGCGGGTT-3′. They were first cloned into pcDNA3.1/V5-His-TOPO vector (Invitrogen), and then subcloned into the sites of KpnI and XhoI of pGL4.23(*luc2*/minP) vector (Promega). Similarly, the mouse ASPP2 promoter sequence −765 to −608 has been amplified from mouse genomic DNA by PCR using the forward primer 5′-ACTACTGCCAATTTCCCAGC-3′ and reverse primer 5′- GTTCAAAACACAGGGAACCC -3′. The same was done for the mouse ASPP2 promoter sequence −645 to −507 with forward primer 5′-AAATCCTTTGAGCGTGCTGT-3′ and reverse primer 5′-GCCTGAGGGATGAGGACAAA-3′. Finally, the putative STAT1 consensus sequence, positioned −590 to −582 on the murine promoter, was removed from the resulting murine −645 to ∼ −507 construct to create the Δ(−590 to ∼ −582) construct by PCR-driven overlap extension using partial overlapping primers: 5′-TAAGAAGGGACAGTGTTGAGAAGTGGGGGGGTTCCCTGTG-3′ and 5′-CTCAACACTGTCCCTTCTTACATTATAGAAGTAACAGGCC-3′.

Luciferase Assay. HEK 293T cells were plated in 24-well tissue culture plates and maintained in medium for 24 h. Cells were transfected using Lipofectamine 2000 (Invitrogen) with the indicated amounts of the plasmids or luciferase reporters listed in Table S5. All cells were also transfected with *Renilla* control plasmid to normalize transfection efficiencies. After transfection, cells were left overnight. The next day, cells were either left untreated or incubated with the indicated amount of ligand. After the indicated treatment period, cells were harvested in passive lysis buffer and assayed for luciferase activity per the manufacturer's protocol.

Statistical Analysis. Data are presented as mean ± SEM. Statistical comparisons were made using the Student *t* test. Differences were considered significant at a value of $^{*}P \leq 0.05$, $^{**}P \leq 0.01$, or $^{***}P \leq 0.001$. Image J software was used to quantify gel bands from immunoblots by densitometry.

1. Vives V, et al. (2006) ASPP2 is a haploinsufficient tumor suppressor that cooperates with p53 to suppress tumor growth. *Genes Dev* 20(10):1262–1267.
2. Young CC, et al. (2013) Ependymal ciliary dysfunction and reactive astrocytosis in a reorganized subventricular zone after stroke. *Cereb Cortex* 23(3):647–659.
3. Barber PA, Hoyte L, Colbourne F, Buchan AM (2004) Temperature-regulated model of focal ischemia in the mouse: A study with histopathological and behavioral outcomes. *Stroke* 35(7):1720–1725.
4. Goings GE, et al. (2008) Hematopoietic cell activation in the subventricular zone after Theiler's virus infection. *J Neuroinflammation* 5:44.
5. Oleszak EL, Chang JR, Friedman H, Katsetos CD, Platsoucas CD (2004) Theiler's virus infection: A model for multiple sclerosis. *Clin Microbiol Rev* 17(1):174–207.
6. Stolp HB, et al. (2011) Reduced ventricular proliferation in the foetal cortex following maternal inflammation in the mouse. *Brain* 134(Pt 11):3236–3248.
7. Notari M, et al. (2011) Inhibitor of apoptosis-stimulating protein of p53 (iASPP) prevents senescence and is required for epithelial stratification. *Proc Natl Acad Sci USA* 108(40):16645–16650.

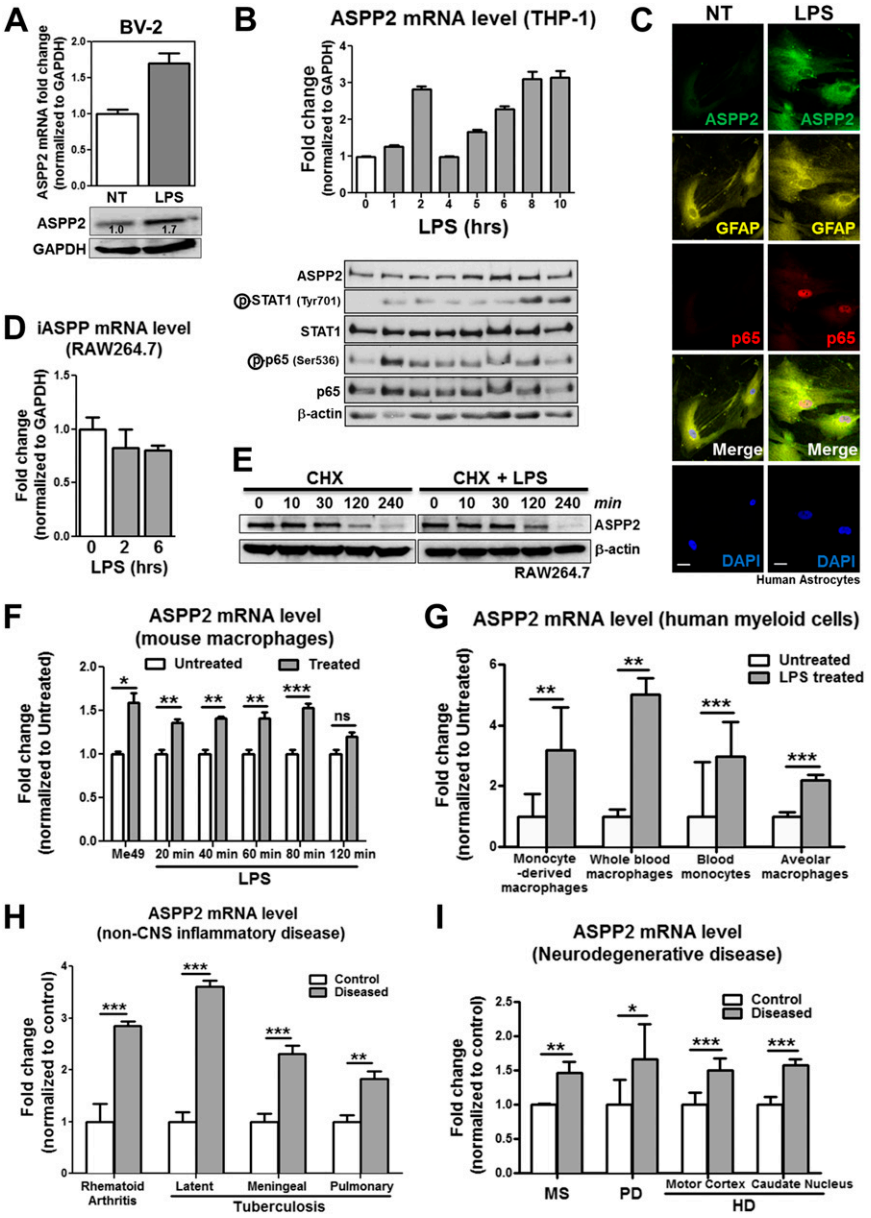

Fig. S1. ASPP2 is induced by LPS. (*A*) ASPP2 mRNA and protein levels are induced in BV-2 cells after LPS treatment. (*B*) LPS time course showing increased ASPP2 expression at the protein and mRNA levels in THP-1. Expression levels of signaling pathways downstream of LPS were examined, including STAT1 and p65. (*C*) ASPP2 is induced in primary human astrocytes in the cytoplasm in a pattern overlapping the intermediate filament GFAP. (Scale bar: 10 μm.) (*D*) iASPP mRNA is not induced after LPS treatment in RAW264.7 cells. (*E*) Cycloheximide (CHX) treatment with or without LPS treatment in RAW264.7 cells. Previously published gene array data showing ASPP2 mRNA expression levels in (*F*) mouse macrophages treated with Me49 (1) and LPS at various time points compared with controls (2); (*G*) human monocyte-derived macrophages (3), whole blood (4), blood monocytes (5), and alveolar macrophages (6) treated with LPS compared with controls; (*H*) inflamed/infected macrophages from patients with (*i*) rheumatoid arthritis (7), (*ii*) latent tuberculosis (8), (*iii*) meningeal tuberculosis (15), or (*iv*) pulmonary tuberculosis (8) compared with control macrophages; and (*I*) brain tissues from patients with neurodegenerative diseases [multiple sclerosis (MS) (9), Parkinson disease (PD) (10), Huntington disease (HD; motor cortex), and HD (caudate nucleus) (11)] compared with control brain tissue. NT, no treatment. $*P \leq 0.05$. $**P \leq 0.01$. $***P \leq 0.001$.

1. Jensen KD, et al. (2011) Toxoplasma polymorphic effectors determine macrophage polarization and intestinal inflammation. *Cell Host Microbe* 9(6):472–483.
2. Ramsey SA, et al. (2008) Uncovering a macrophage transcriptional program by integrating evidence from motif scanning and expression dynamics. *PLOS Comput Biol* 4(3):e1000021.
3. Schroder K, et al. (2012) Conservation and divergence in Toll-like receptor 4-regulated gene expression in primary human versus mouse macrophages. *Proc Natl Acad Sci USA* 109(16):E944–E953.
4. Wurfel MM, et al. (2005) Identification of high and low responders to lipopolysaccharide in normal subjects: An unbiased approach to identify modulators of innate immunity. *J Immunol* 175(4):2570–2578.
5. Dower K, Ellis DK, Saraf K, Jelinsky SA, Lin LL (2008) Innate immune responses to TREM-1 activation: Overlap, divergence, and positive and negative cross-talk with bacterial lipopolysaccharide. *J Immunol* 180(5):3520–3534.
6. Reynier F, et al. (2012) Gene expression profiles in alveolar macrophages induced by lipopolysaccharide in humans. *Mol Med* 18:1303–1311.
7. Koulouvaris P, et al. (2008) Expression profiling reveals alternative macrophage activation and impaired osteogenesis in periprosthetic osteolysis. *J Orthop Res* 26(1):106–116.
8. Thuong NTT, et al. (2008) Identification of tuberculosis susceptibility genes with human macrophage gene expression profiles. *PLoS Pathog* 4(12):e1000229.
9. Padden M, et al. (2007) Differences in expression of junctional adhesion molecule-A and beta-catenin in multiple sclerosis brain tissue: Increasing evidence for the role of tight junction pathology. *Acta Neuropathol* 113(2):177–186.

10. Zhang Y, James M, Middleton FA, Davis RL (2005) Transcriptional analysis of multiple brain regions in Parkinson's disease supports the involvement of specific protein processing, energy metabolism, and signaling pathways, and suggests novel disease mechanisms. *Am J Med Genet B Neuropsychiatr Genet* 137B(1):5–16.
11. Hodges A, et al. (2006) Regional and cellular gene expression changes in human Huntington's disease brain. *Hum Mol Genet* 15(6):965–977.

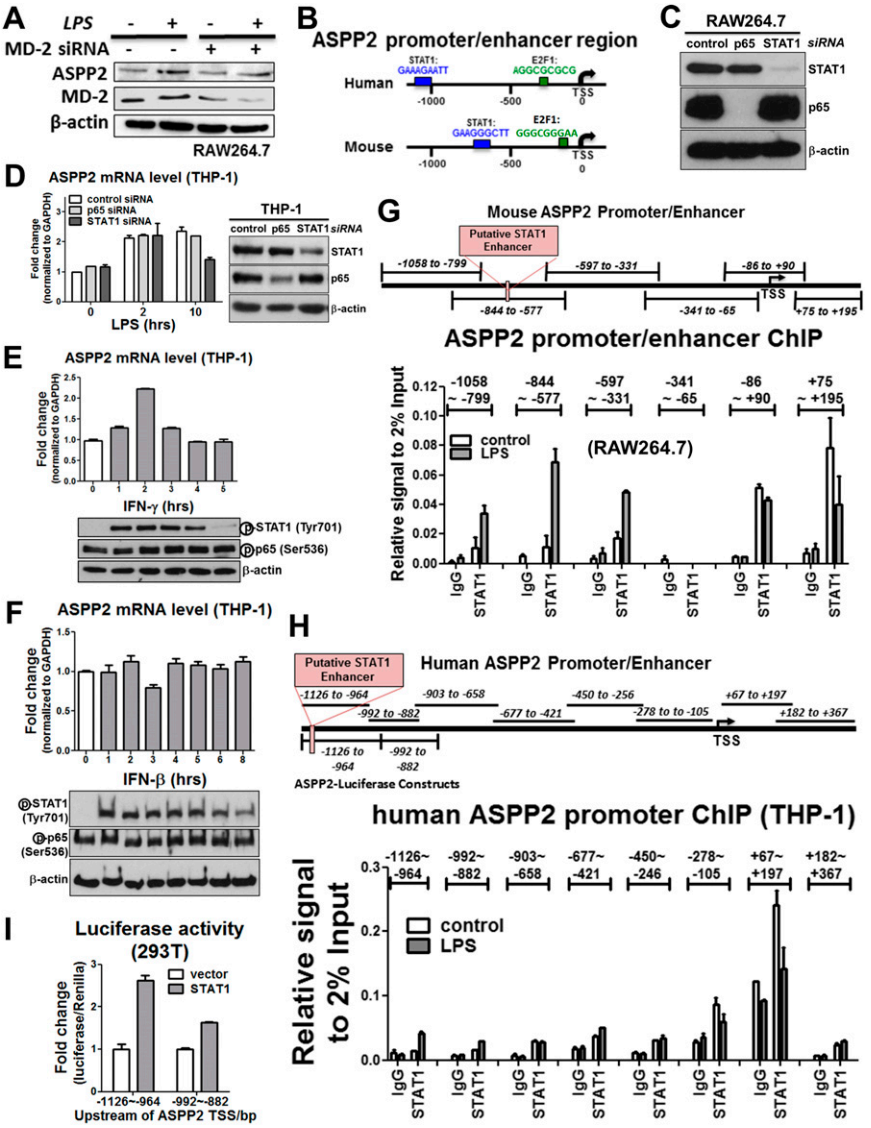

Fig. S2. ASPP2 is a target of STAT1. (*A*) siRNA of MD-2 reduces ASPP2 induction after LPS treatment in RAW264.7 cells. (*B*) Illustration of the human and mouse ASPP2 promoter/enhancer region with putative STAT1 binding site and published E2F1 binding site (1). (*C*) Western blot showing knockdown efficiency of p65 and STAT1 in RAW264.7 cells. (*D*) Expression of ASPP2 mRNA was examined with siRNA of p65 or STAT1 with or without LPS treatment at 2 or 10 h in THP-1 cells. Only STAT1 siRNA diminished the induction of ASPP2 after LPS at 10 h. Western blot showing knockdown efficiency of p65 and STAT1 in THP-1 cells. (*E*) IFN-γ induces ASPP2 mRNA expression in THP-1 cells but (*F*) IFN-β fails to do so. Expression levels of signaling pathways downstream of LPS were examined, including STAT1 and p65. (*G*) Illustration of the mouse ASPP2 promoter/enhancer region from 1,058 bp upstream of the TSS to 195 bp downstream of the TSS. Putative STAT1 binding site is shown. Results of the STAT1 ChIP in RAW264.7 cells across the promoter/enhancer region of the mouse ASPP2 gene. The regions corresponding to each of the primer sets are shown. Results are the average of duplicate treatments, and error bars show the range of the duplicates. (*H*) Illustration of the human ASPP2 promoter/enhancer region from 1,126 bp upstream of the TSS to 367 bp downstream of the TSS. Putative STAT1 binding site is shown. Results of STAT1 ChIP in THP-1 cells across the promoter/enhancer region of the human ASPP2 gene. The regions corresponding to each of the primer sets are shown. Results are the average of duplicate treatments, and error bars show the range of the duplicates. The −1,126 to −882 region of the ASPP2 enhancer/promoter region is maximally responsive to LPS. (*I*) Exogenous expression of STAT1 activates ASPP2 (−1,126 to −964) -Luc and ASPP2 (−992 to −882) -Luc activity in 293T cells.

1. Fogal V, et al. (2005) ASPP1 and ASPP2 are new transcriptional targets of E2F. *Cell Death Differ* 12(4):369–376.

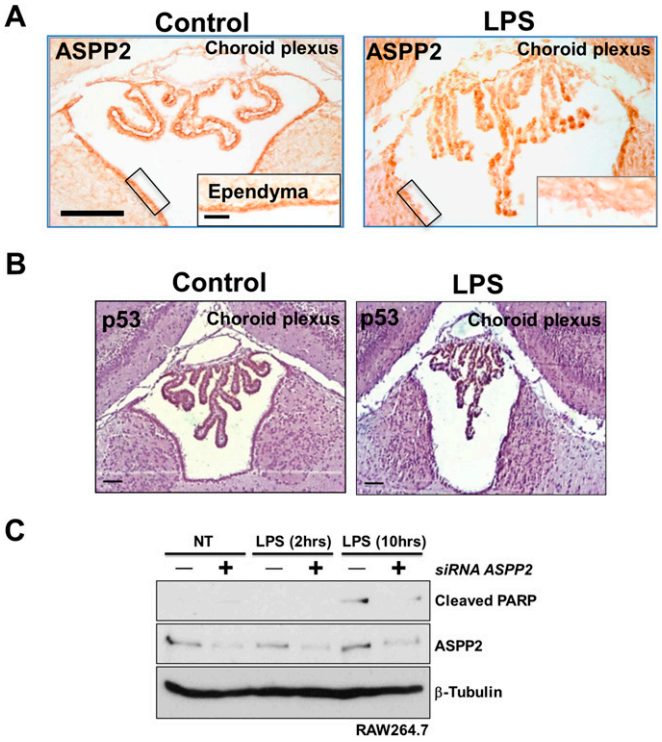

Fig. S3. LPS induces nuclear ASPP2 expression in a model of maternal inflammation, and ASPP2 mediates apoptosis. (*A*) ASPP2 is induced and relocalized to the nucleus from the tight junctions of choroid plexus epithelial cells but not the ependymal cells lining the third ventricle. (Scale bar: 100 μm; *Insets*, 25 μm.) (*B*) After LPS injection, p53 appears in the nucleus of choroid plexus epithelial cells. (Scale bars: 50 μm.) (*C*) ASPP2 knockdown reduces cleaved PARP expression after 10 h of LPS treatment in RAW264.7 cells. NT, no treatment.

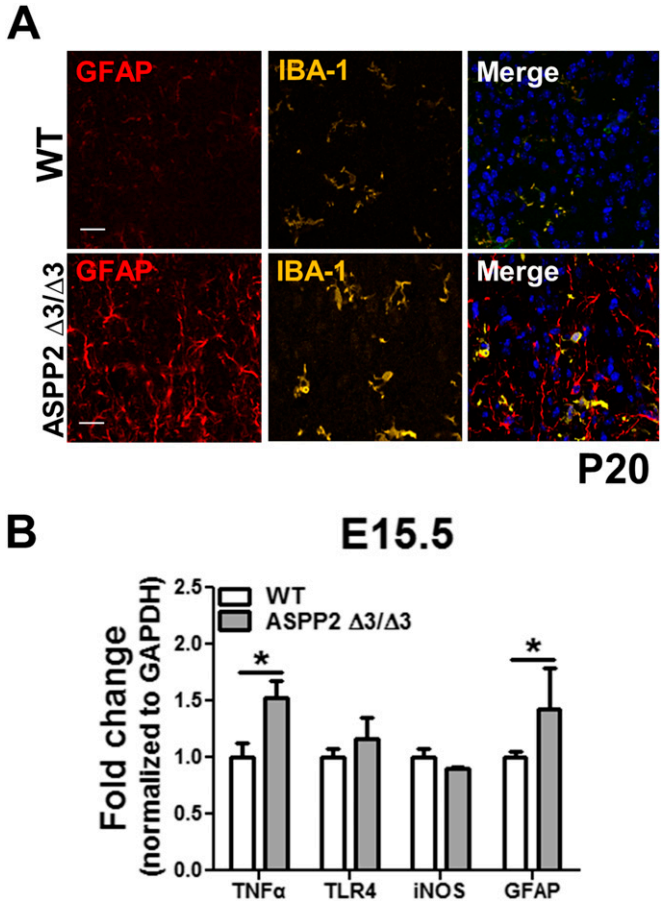

Fig. S4. ASPP2-deficent mice possess neuroinflammation. (*A*) Increased IBA1-positive microglia and GFAP-positive astrocytes in ASPP2 Δ3/Δ3 mice at postnatal day 20 (P20). (Scale bars: 10 μm.) (*B*) Increased proinflammatory cytokines in cortical brain tissue of ASPP2 Δ3/Δ3 mice at embryonic day 15.5 (E15.5). *$P \leq 0.05$.

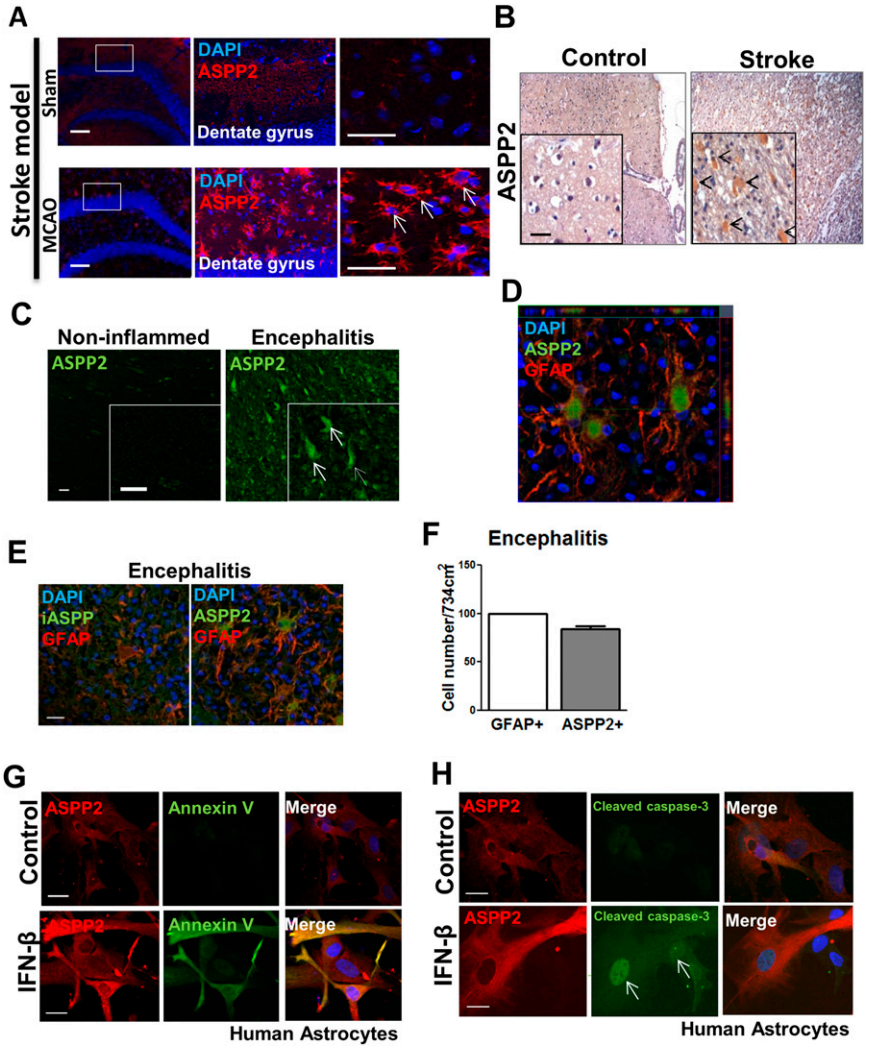

Fig. S5. ASPP2 up-regulation in mouse models and human neuroinflammatory disorders. (*A*) ASPP2 is up-regulated in the middle cerebral artery occlusion (MCAO) in stroke model animals compared with sham operated controls in cells with an astrocyte morphology in the hippocampus. (Scale bar: 25 μm; *Insets*, 10 μm.) Increased ASPP2 expression in cells with astrocyte morphology (arrows) in (*B*) cerebral ischemia and (*C*) encephalitis. (Scale bar: 25 μm; *Insets*, 10 μm.) (*D*) Orthogonal plane of ASPP2-expressing astrocytes in encephalitis tissue shows that ASPP2 is localized to the cytoplasm. (Scale bar: 10 μm.) (*E*) iASPP is not highly expressed in astrocytes in encephalitis tissue. (Scale bar: 10 μm.) (*F*) About 85% of ASPP2-expressing cells also coexpress GFAP. (*G*) Annexin V or (*H*) cleaved caspase-3 immunocytochemistry staining of human astrocytes after 24 h IFN-β treatment. (Scale bar: 25 μm.)

Table S1. Primary antibodies

Antigen	Name	Source	Application
Caspase-3	—	Cell Signaling	WB
Cleaved caspase-3	—	Cell Signaling	WB, IF, ICC
Cleaved PARP	—	Cell Signaling	WB
GFAP	—	Abcam	IF, ICC
GFP	—	Abcam	WB
IBA-1	—	Wako	IF, IHC
LX116	ASPP2	Ascites	IHC
LX49.3	iASPP	Ascites	IF
p53	CM5	Leica	IHC
RELA/p65	A, F-6	Santa Cruz	ICC
RELA/p65	Active subunit, 12H11	Millipore	WB
S32	ASPP2	Serum	WB
STAT1	M-23	Santa Cruz	IF, ICC
Toll-like receptor 4	—	Abnova	WB
MD-2	—	Abcam	WB
Phospho-STAT1 (Tyr701)	58D6	Cell Signaling	WB
Phospho-p65 (Ser536)	93H1	Cell Signaling	WB
Lamin B	—	Cell Signaling	WB
β-Actin	C-20	Santa Cruz	WB
β-Tubulin	—	Abcam	WB

ICC, immunocytochemistry; IF, immunofluorescence; IHC, immunohistochemistry; WB, Western blot.

Table S2. Secondary antibodies

Antibody name	Host/type	Source	Applications
Alexa Fluor 488 anti-rabbit IgG	Goat	Invitrogen	IF, ICC
Alexa Fluor 488 anti-mouse IgG	Goat	Invitrogen	IF, ICC
Alexa Fluor 546 anti-rabbit IgG	Goat	Invitrogen	IF, ICC
Alexa Fluor 546 anti-chicken IgG	Goat	Invitrogen	IF
Alexa Fluor 546 anti-mouse IgG	Goat	Invitrogen	IF, ICC
Alexa Fluor 647 anti-mouse IgG	Donkey	Invitrogen	IF
Anti-mouse Igs/HRP	Rabbit	Dako	WB
Anti-rabbit Igs/HRP	Swine	Dako	WB
Biotinylated anti-mouse IgG	Goat	Vector Laboratories	IHC
Biotinylated anti-rabbit IgG	Goat	Vector Laboratories	IHC

ICC, immunocytochemistry; IF, immunofluorescence; IHC, immunohistochemistry; WB, Western blot.

Table S3. Primers for quantitative RT-PCR

Transcript name/direction	Sequence (5′ to 3′)
TNF-α	
Forward	TCTCATCAGTTCTATGGCCC
Reverse	GGGAGTAGACAAGGTACAAC
GFAP	
Forward	ACACCAGCACTTCCCTTCCTTC
Reverse	TCTGCTCATCTTTCCTCTTCCC
iNOS	
Forward	CCCTTCCGAAGTTTCTGGCAGCAGC
Reverse	GGCTGTCAGAGAGCCTCGTGGCTTTGG
IL-1β	
Forward	TTGACGGACCCCAAAAGATG
Reverse	AGAAGGTGCTCATGTCCTCA
GAPDH	
Forward	TGTCAGCAATGCATCCTGCA
Reverse	TGTATGCAGGGATGATGTTC

Primers in the table were purchased from Eurofins. Primers for human ASPP2, mouse ASPP2, and mouse iASPP were purchased from Qiagen (sequences available from Qiagen).

Table S4. Primers for ChIP

Species	5′ ASPP2 promoter position (TSS)	3′ ASPP2 promoter position (TSS)	Direction	Sequence (5′ to 3′)
Human	−1,126	−964	Forward	TCGATGGAGATTCTGGTAAGGG
			Reverse	TGTTCTAGTAAGTTGTCAGTGCA
Human	−992	−882	Forward	TGAACTTGCACTGACAACTTACT
			Reverse	AAAGAGTAGCAGAGCGGGTT
Human	−903	−658	Forward	TGAACCCGCTCTGCTACTCT
			Reverse	CAAACGTACACCGCAAACTG
Human	−677	−421	Forward	CAGTTTGCGGTGTACGTTTG
			Reverse	AGAGAGGCGGACGGACTT
Human	−450	−246	Forward	GGGCCTCCCCTGAAGTC
			Reverse	CCTCAGGAAAACAGGATGGT
Human	−278	−105	Forward	GGTGCCATTCACTACCATCC
			Reverse	GGCCCGGCTGGGTAGAC
Human	67	197	Forward	GAGCGTCGAAGAGACAAAGC
			Reverse	AAGCGGGTGGCCAGACT
Human	182	367	Forward	CCGCCTCGCAACAGGTC
			Reverse	CGACCCCGCACACTTCC
Murine	−1,058	−799	Forward	TTATCCAGAGAGACATAGGCTTCA
			Reverse	AGGTCTTACTCTTTCAGCTCAGG
Murine	−844	−577	Forward	GGGAAAAGCCCTTCAGTGTTG
			Reverse	AGCTTCGTGGAGTTAGTGTTCC
Murine	−597	−331	Forward	AGCCCTTTGCCTTAGGAACC
			Reverse	CAACACTGAAGGGCTTTTCCC
Murine	−341	−65	Forward	CAAGGCTTGAGGTAAGGGGG
			Reverse	GGCAAAGGGCTCAACTCTCT
Murine	−86	90	Forward	AATCCCCTCGCCCGTCTC
			Reverse	CTCCCCCTTACCTCAAGCCT
Murine	75	195	Forward	GGAAGCCAAGCGAGAACGAG
			Reverse	GACGGGCGAGGGGATTG
Murine	−765	−608	Forward	ACTACTGCCAATTTCCCAGC
			Reverse	GTTCAAAACACAGGGAACCC
Murine	−645	−507	Forward	AAATCCTTTGAGCGTGCTGT
			Reverse	GCCTGAGGGATGAGGACAAA
Murine	−557	−398	Forward	ACAGGCCATTCAGAGGGG
			Reverse	TGAGTCAGGTGTGTGAGGC

Table S5. Plasmids

Name	Vector	Information	Source
TLR4	pcDNA3.1	Human TLR4	Doug Golenbock
Control plasmid	pcDNA3.1	Empty vector	Invitrogen
RELA/p65	pcDNA3.1	Human p65	Nancy Rice
STAT1	pcDNA3.1	Human STAT1	S.N.C.

TLR4, toll-like receptor 4.